Impact of the Alkali Cation on the Oscillatory Electro-Oxidation of Ethylene Glycol on Platinum

Elton Sitta,*[†,‡] Raphael Nagao,[§] István Z. Kiss,[§] and Hamilton Varela*[†]

[†]Institute of Chemistry of São Carlos, University of São Paulo, CP 780, CEP 13560-970, São Carlos, São Paulo, Brazil
[‡]Department of Chemistry, Federal University of São Carlos, CP 676, CEP 13565-905, São Carlos, São Paulo, Brazil
[§]Department of Chemistry, Saint Louis University, 3501 Laclede Avenue, St. Louis, Missouri 63103, United States

ABSTRACT: We report the effect of alkali cation (Li^+, Na^+, and K^+) on the oscillatory electro-oxidation of ethylene glycol in alkaline media. As experimentally verified, the nature of the alkali cation strongly impacts the waveform and frequency of the potential oscillations. The oscillation frequencies decrease in the order KOH > NaOH > LiOH, which also corresponds to the ascending order of the surface blockage due to the noncovalent interactions. On the other hand, the estimated rate constant of poison formation, k_p, under oscillatory regime is higher in the presence of KOH rather than NaOH, both acting as the supporting electrolytes. In order to shed light on the relationships between the kinetic and dynamical features, we performed numerical simulations based on a generic model which includes the time evolution of cation coverage. Overall, we were able to reproduce the major features observed experimentally; k_p was assigned to the electrochemical steps of C−C bond breaking instead of direct noncovalent interactions between the hydrated alkali cation and surface oxides. Finally, the results are rationalized in terms of the cation influence on the feedback loops and of the underlying surface chemistry.
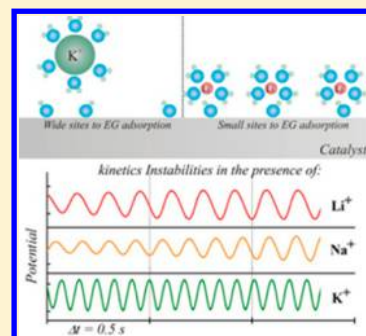
1. INTRODUCTION

It is well-known that adsorbing anions play an important role in many electrochemical reactions in acidic media.[1,2] Because of the specific adsorption, these species can block active sites and/or drive the reaction through different pathways.[3−6] Cations can also affect the rates of surface reactions, however, the effect cannot be straightforwardly explained as in the case of electrosorbing anions. Markovic et al.[7] rationalized this phenomenon by means of noncovalent interaction between cations, at the outer Helmholtz plane, and negatively charged adsorbed species. Because of the electrostatic nature, the interaction strength increases with the charge density of the cation and its influence on overall dynamics depends on the nature of both the cation and negatively adsorbed species at surface. For example, the surface poisoning effect of PtOH−$M^+(H_2O)_x$ clusters at the interface decreases in the order of the hydration energy of the alkali metal M, $Li^+ > Na^+ > K^+ > Cs^+$, and the catalytic activity usually increases from Li^+ to Cs^+. Similar inhibition trends have been found in the electro-oxidation of hydrogen,[7] carbon monoxide,[8] formic acid,[9] methanol,[7] ethylene glycol,[10] and glycerol[11] and in the electro-reduction of oxygen[7] and hydrogen peroxide[12] on platinum. Recently, DFT calculations provided evidence of alkali cation specific adsorption[13] and respective competition with hydrogen ions for active sites[14] on well oriented platinum surfaces.

For the electrocatalytic oxidation of ethylene glycol (EG) on platinum, the increase of the strength of noncovalent interactions (on the alkaline series K^+, Na^+, and Li^+) was found to enhance the inhibiting effect and to make it more

difficult to break the C−C bond.[10] The reaction cited above shows dynamic instabilities observed as potential or current oscillations in time, depending on the controlled parameter. Generally speaking, oscillatory behavior during the electro-oxidation of small organic molecules results from the competition between adsorption isotherms of electro-active species and of poisoning intermediates, being the last associated with the presence of adsorbed residues of main reaction, usually referred to as CO, on platinum surfaces and acid media.[15−17] These reactions are classified as hidden negative differential resistance (HN-NDR) oscillations because the negative differential resistance (NDR) of the inhibiting steps on the current vs potential profile is hidden in a slow potential sweep due to the presence of parallel reactions with positive differential resistances.[18] HN-NDR oscillations occur under both current and potential control; under potentiostatic control the system requires a critical ohmic drop, usually obtained by insertion of an external resistance in series with the working electrode. The HN-NDR systems remain oscillatory for any external resistance larger than the critical value in the appropriate range of circuit potentials.[15] We found that the features of oscillations are rather sensitive to parameters such as temperature and pH.[19−21] EG electro-oxidation in alkaline media shows potential and current oscillations with frequencies at least 10 times faster than those found for comparable systems.[22,23] Besides, electro-catalytic oscillators of the HN-NDR-type are sensitive to the
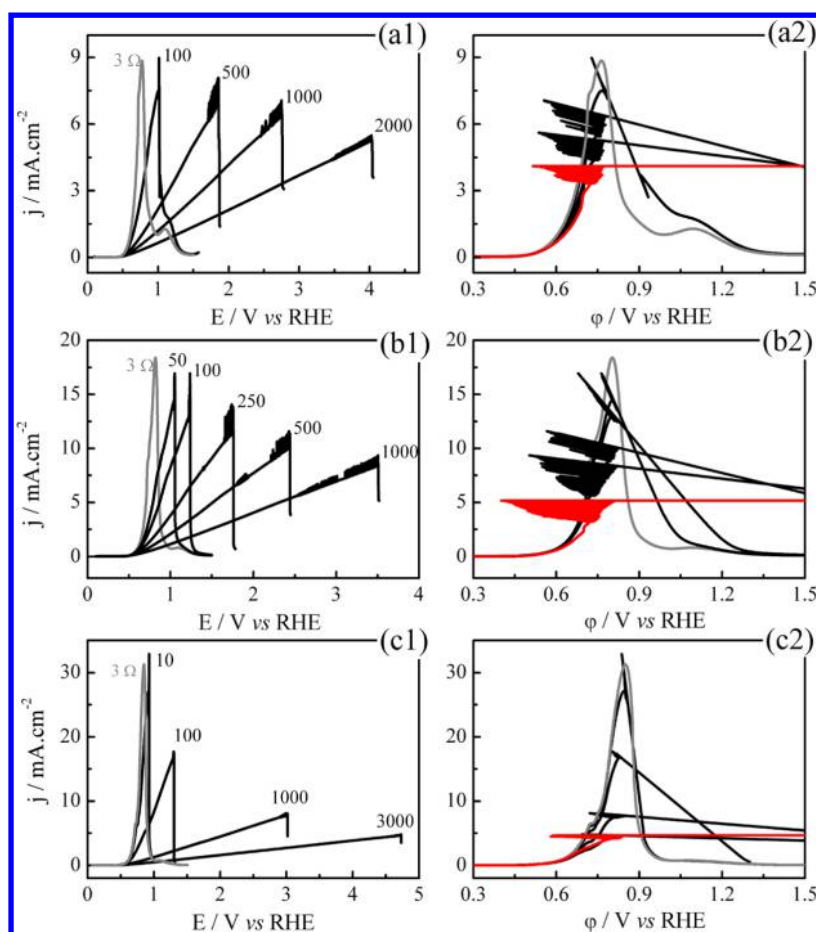
Figure 1. (1) Linear potential sweeps, at $dE/dt = 0.01$ V s^{-1}, in the presence of different external resistances connected in series with the working electrode and (2) the potential after the ohmic drop correction. Red lines represent the potential registered along a galvanodynamic sweep at $dj/dt = 4$ μA cm^{-2} s^{-1}. Electrolyte is [EG] = 0.5 mol L^{-1} in aqueous [MOH] = 1.0 mol L^{-1}, with M of (a) Li, (b) Na, and (c) K.

nature of electrosorbing species present in the electrolyte. All studies on this direction, however, are concerned with the influence of anions on the dynamics.[24−27]

In this work, we explore the effect of the alkali cations on the complex routes of EG electro-oxidation by studying the nonlinear kinetics of the reaction in aqueous KOH, NaOH, and LiOH solutions. The comparison of the dynamical responses in the presence of the different alkali cations reveals their importance for both the qualitative and the quantitative features of the nonlinear behavior. In addition to experiments, we have also investigated the system numerically with a generic model that accounts for the cation inhibition.

2. EXPERIMENTAL SECTION

All experiments were developed in a standard three-electrode electrochemical cell, with temperature control fixed at 20 °C. The working electrode consists of a Pt band with 0.27 cm^2 in area, measured by hydrogen OPD charge, considering 210 μC per cm^2. As counter electrode, a platinized Pt band with high area was employed (more than 2000× the area of the working electrode), and all potentials were measured and quoted with respect to the reversible hydrogen electrode (RHE), prepared with the same solution of the supporting electrolyte. The supporting electrolyte was prepared by the dissolution of MOH (M = Li, Na, or K) in Milli-Q water (18.2 MΩ cm) in sufficient amount to give a concentration of 1.0 mol L^{-1} and further addition of 0.5 mol L^{-1} ethylene glycol (J. T. Baker). High

purity hydroxides (at least 99.99%) were provided by Fluka (monohydrated LiOH) and Sigma-Aldrich (NaOH and KOH).

Before the addition of ethylene glycol to the cell, the cleanness of the system was attested by signature of a clean platinum voltammetric profile registered at 0.05 V s^{-1} between hydrogen and oxygen evolution regions. The protocol followed before every measurement was the following: clean the electrode in a butane/air flame, and cool the surface on cell atmosphere. Inserting the electrode polarized at 0.05 V, and perform five potential cycles between 0.05 and 1.50 at 0.1 V s^{-1}. More details of the experimental protocol can be found in a previous publication.[10] The increase of ohmic resistance was made through a resistance box (Minipa) placed between the Pt (working) electrode and working point of the potentiostat (AutoLab 302N). The electrochemical study was performed by means of potentio/galvanodynamic sweeps and of stationary experiments under both forms of control. Under potentiostatic regime and in the presence of series resistance, the electrode potential, φ, was obtained after subtracting the ohmic drop, IR (or jAR; vide infra) from the applied voltage; i.e. $\varphi = E - IR$. Under galvanostatic regime, E and φ become equivalent.

3. RESULTS AND DISCUSSION

3.1. Experiments. The left column of Figure 1 (parts a1, b1, and c1) shows the linear potential sweeps for the electro-oxidation of ethylene glycol in the presence of different cations and external resistances, a, b, c being the curves corresponding

to the electrolytes containing Li$^+$, Na$^+$, and K$^+$, respectively. The base curves without external resistance are subjected only to solution resistance of 3 Ω and are presented in gray. The peak current amounts to 9, 17, 31 mA cm^{-2} for Li$^+$, Na$^+$, and K$^+$ ions, respectively. The difference in activity is a direct effect of the surface blockage which decreases in the same sequence and is also related to the extent of scission of the C−C bond.[10] In all three supporting electrolytes the increase of ohmic resistance affected the dynamical behavior and current oscillations were observed during linear potential sweeps at sufficiently large external resistances. Because of the external resistance, the applied potential/voltage (E) differs from the electrode potential (φ), the last being revealed after subtraction of ohmic drop (product of external resistance and current). The right column in Figure 1 (parts a2, b2, and c2) shows the curves of the left side after *IR* correction, including also the galvanodynamic sweeps at dj/dt = 4 μA cm^{-2} s^{-1}, in red. As the resistance increases, the potentiodynamic sweeps approach this profile, indicating that effective (interface) potential becomes independent of the applied potential.

Figure 2 shows a set of selected potentiostatic time series collected at different resistances for the electro-oxidation of EG in the three electrolytes investigated, giving special attention to the beginning of oscillatory cycle in each series, i.e., near Hopf
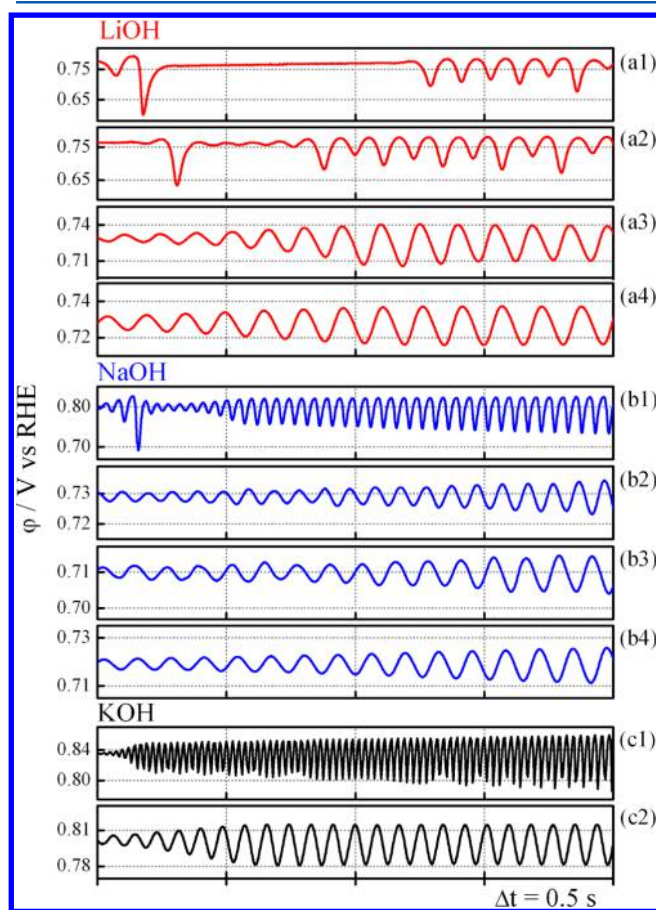

Figure 2. Oscillatory time series during the electro-oxidation of ethylene glycol in the presence of different alkali cations (M) and distinct external resistances: (a1) 150 Ω; (a2) 250 Ω; (a3) 3000 Ω; (a4) galvanostatic j = 3.62 mA cm^{-2}; (b1) 50 Ω; (b2) 1000 Ω; (b3) 3000 Ω; (b4) galvanostatic j = 3.12 mA cm^{-2}; (c1) 12 Ω; (c2) galvanostatic j = 4.18 mA cm^{-2}. Electrolyte is [EG] = 0.5 mol L^{-1} in aqueous [MOH] = 1.0 mol L^{-1}, with M = Li, Na, and K.

bifurcation. The applied potentials were chosen with basis on potential sweeps showed in Figure 1 (left column) for each condition of resistance and cation. For KOH electrolyte, only lower resistances and galvanostatic series were depicted, i.e., series c1 and c2; the complete time series can be found in ref 28. With potassium, the typical waveform at the oscillation onset is relatively simple period 1 oscillations and seems to be resistance independent. When potassium ions are replaced by lithium (series a1−a4) or sodium ions (series b1−b4), more complex waveform patterns can be observed with some resistances, for instance, with 250 and 500 Ω in Na$^+$ containing electrolyte, not shown, or at resistances lower than 1000 Ω in LiOH solutions (series a1 and a2). When KOH is used as supporting electrolyte, oscillations are generally more complex as the time series spontaneously evolves, and this is particularly true at high resistances and under galvanostatic control.

In any case, the oscillation frequency was found to increase with cation size and thus with the decrease of population of interfacial PtOH−M$^+$(H$_2$O)$_x$ clusters. Period 1 oscillations obtained under galvanostatic regime have the frequencies of 6.8, 7.7, and 10 Hz for electrolytes containing Li$^+$ (a4), Na$^+$ (b4), and K$^+$ (c2), respectively.

Changes in the features of oscillation are common in acidic media as a result of the presence of electrosorbing anions. The competition for surface sites impacts the availability of adsorbed species so that anions with high adsorption strength, such as Cl$^-$, can strongly modify the oscillatory waveforms. Examples can be found during electro-oxidation of CO[29,30] or formic acid.[25−27,31] The presence of halogen ions during electro-reduction of hydrogen peroxide can extinguish or create new type of oscillations regions.[32] Our previous report on the oscillatory electro-oxidation of methanol on platinum and in acidic media[24,33] indicated that the oscillation frequency remains nearly unaffected by surface blockage caused by anion adsorption, but a slight decrease could be detected in the oscillatory frequency as a result of anion adsorption. This observation is in line with the frequency decrease due to the increase in the interfacial concentration of PtOH−M$^+$(H$_2$O)$_x$ clusters found here. An additional aspect to be compared is the effect of surface blockage on the general stability of the electrochemical oscillations as inferred by the duration of the time series. For the methanol system in acidic media[24] it was found that anion adsorption strongly impacts the duration of the time series; in contrast, with these cations, we did not find a clear pattern for the effect of the concentration of PtOH−M$^+$(H$_2$O)$_x$ clusters at the interface on the stability of the oscillations (data not shown). These aspects are, in fact, connected to some mechanistic differences between the two types of inhibition.

In general terms there are two important differences in the site blockage in alkaline media when compared to that caused by anion adsorption in acidic media. First, there is an inverse potential dependence: in alkaline media, although the cation coverage can be favored by the formation of platinum oxides, surface poisoning decreases with high potential values because of electrostatic repulsion between positively charged surface and cations; in acidic media the blockage increases monotoni-cally with the electrode potential. Second, besides surface poisoning, the noncovalent interactions, between adsorbed oxygenated species and hydrated alkali cations, make the adsorbed oxygenated species unavailable for oxidizing carbona-ceous adsorbates. Therefore, it seems clear that the presence of PtOH−M$^+$(H$_2$O)$_x$ clusters has a more delicate influence on the

surface chemistry than simply blocking surface sites. Since oscillations result from the coupling among different reaction steps with specific potential dependencies, the influence of interfacial $PtOH-M^+(H_2O)_x$ clusters on the main reaction seems to occur in a nontrivial mechanism. In the following, we further analyze some aspects of these effects.

Kiss et al.[28,34] developed a relation between the oscillation frequency and the external resistance of the system. By use of generic equations for electrochemical oscillations, a relationship was found between the frequency of the oscillations and some kinetic parameters,

$$\omega = \frac{1}{2\pi} \sqrt{\frac{k_{p,e}}{C_{DL}}\left(\frac{1}{RA} + \frac{dj}{d\varphi}\right)}\bigg|_{\varphi = \varphi_{Hopf}} \quad (1)$$

where φ_{Hopf} is the Hopf potential, where the oscillations set in; ω is the oscillation frequency; $k_{p,e}$ is the first order poisoning rate measured experimentally; C_{DL} is the double layer capacitance per unit area; R is the total system resistance (solution plus external resistances); A is the electrode area; and $dj/d\varphi$ is the first derivative of current density vs potential curve obtained under potentiodynamic regime. This relation is satisfactorily observed for oscillatory nickel electro-dissolution in acid media and EG electro-oxidation reaction in KOH.[28] The main feature of this equation is the possibility to infer about the surface poisoning without previous considerations concerning the reaction mechanism.[35,36]

With the focus of our analysis on series in which only simple period 1 oscillations are observed, Figure 3a shows the dependence of the oscillation frequency on the applied external resistance. ω represents the mean frequency during the first

Figure 3. (a) Oscillatory frequency as a function of the total resistance and for the galvanostatic case (dashed lines). (b) Relation between oscillatory frequency and total resistance according to eq 1. Data were taken from series similar to that shown in Figure 2.

second of the oscillations with the error bars expressing the standard deviations. The presence of Li^+ or Na^+ instead of K^+ in the supporting electrolyte decreases ω in all resistance ranges. Dotted lines represent ω value obtained under galvanostatic control, highlighting the convergence of values when R and E go simultaneously to infinity. The linearized plot of the frequency, as given in eq 1, shows a relatively good fit to the experimental data. For lithium it was not possible to obtain the graph, since there was only one series with period 1 oscillations under potentiostatic control. According to eq 1, the slope of this graph is equal to $k_{p,e}/(4\pi^2 C_{DL})$. By means of ac techniques, the double layer capacitances were estimated as 34.3 and 40.9 $\mu F\ cm^{-2}$ for the systems containing Na^+ and K^+ ions, respectively. By use of these values and the slope of the graph, poisoning rate constants of 4.5 and 10 s^{-1} were found for the oscillatory EG electro-oxidation in NaOH and KOH aqueous solutions, respectively (the data for K^+ were reported in our previous work[28]). Unfortunately, it is not possible to compare these values with (uncalculated) $k_{p,e}$ for LiOH.

On the basis of the rate constants of surface poisoning just discussed, we can now connect the results on the influence of the nature of the alkali cation under both regular and oscillatory regimes. The currents of EG oxidation are suppressed at low potentials,[10] where there is apparently no inhibition caused by alkali cation.[7,9] It is generally accepted that this poisoning is caused by dissociative adsorption of organic species, suggested as carbonyl species,[37] without a massive oxidation. As the electrode potential increases, these residues are oxidized and free active sites become available. These sites will be occupied by adsorbed EG molecules and $O(H)_x$ (with $x = 0$, 1, or 2) species; among these, the interaction strength of the surface oxide is dependent on the nature of the cation.[7] At high potentials, the surface will be covered by irreversible oxides, mainly PtO, which suppress the overall oxidation current. The oscillatory process develops in the overlapping region of no-EG electro-oxidation and irreversible oxide formation. The maximum potentials reached during oscillations are below the irreversible oxidation of Pt; on the other hand, the minimum potential can be as low as 0.50 V. The potential oscillation window indicates that the poisoning species responsible for the oscillations is eventually some EG oxidation residue/intermediate. In this context, the changes induced by the alkali cation on oscillation patterns and, more specifically, on $k_{p,e}$ are connected with changes in the mechanism of EG electro-oxidation.

We have found that the stronger is the interaction between alkali cations and the platinum oxides on the surface, the lower is the reaction current and the smaller is the production of C1 product, i.e., carbonate, at expense of C2 species, mainly oxalate. Herein we found that cation inhibition causes the decrease of the oscillation frequency and of the poisoning rate constant, $k_{p,e}$ (in the latter, at least when K^+ is replaced by Na^+). In the presence of large cation radius, i.e., K^+, the contradiction between the high overall activity caused the low interfacial concentration of $PtOH-M^+(H_2O)_x$ clusters, under regular regime, and the higher rate of poison formation during oscillations is just apparent and can be tentatively explained as follows. On the one hand, the mentioned inhibition associated by unavailability of interfacial oxygenated species due to the formation of $PtOH-M^+(H_2O)_x$ clusters is likely to influence the oscillations' waveform and frequency. Since the inhibition caused by the alkali cations is essentially identical under both regimes, it becomes clear that an organic residue is
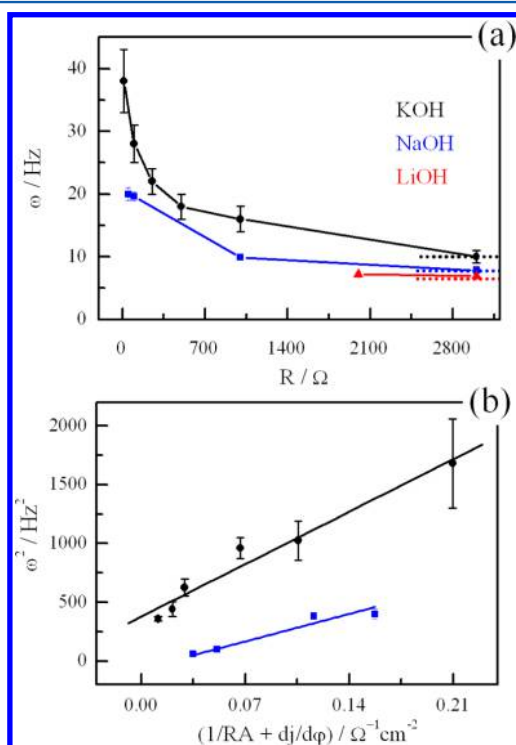
responsible for the poisoning process discussed during oscillations and estimated through eq 1. Despite the complexities and still unknown aspects of the electro-oxidation of EG on platinum, especially in alkaline media, it is indisputable that the oxidation to CO_2, and thus to carbonate, occurs via many surface steps involving adsorbed intermediates such as glyoxal or glycolate.[38] According to our previous report,[10] we found that the complete oxidation to carbonate decreases in the sequence $K^+ > Na^+ > Li^+$. Conversely, the surface blockage, which decreases in the opposite direction, favors desorption of partially oxidized species, for example, oxalate molecules. Therefore, species such as the surface precursor of CO_2/CO_3^{2-} or even the intermediate between the final surface step of conversion between $(COO^-COO^-)_{ad}$ and solution CO_3^{2-} are possible candidates to play a role when the surface is less blocked by noncovalent interactions. Moreover, the relative population of adsorbed organic residues is expected to increase in the sequence $Li^+ < Na^+ < K^+$, similar to the rate of poison formation under oscillatory conditions for Na^+ and K^+. In summary, we found that the noncovalent interactions influence the oscillatory electro-oxidation of ethylene glycol in both feedback loops: the positive one by means of the concentration of $PtOH-M^+(H_2O)_x$ clusters, and the negative one owing to the differences induced in the formation of the adsorbed organic poison. This scenario conciliates the experimental information gathered under conventional[10] and oscillatory regimes presented here and calls for further investigation of the intricate interplay between organic molecules and surface-blocking species at different regimes.

3.2. Numerical Simulations. The numerical investigation was based on a dimensionless electrochemical oscillator of the HN-NDR type,[18] which accounts for the class of systems characterized by a partially hidden (H) negative differential resistance[17] (NDR) in a stationary N-shaped current–potential curve previously formulated by Krischer[39] and based on two electrochemical models originally proposed by Koper and Sluyters.[40,41]

$$\varepsilon\frac{d\phi}{dt} = -c(1-\theta)k + \frac{E-\phi}{\rho} \tag{2}$$

$$\mu\frac{dc}{dt} = -c(1-\theta)k - c + 1 \tag{3}$$

$$\Gamma\frac{d\theta}{dt} = \theta_0 - \theta \tag{4}$$

where k and θ_0 might be described by,[42]

$$k = (2 \times 10^{-5})(\phi^3 - 470\phi^2 + 56000\phi) \tag{5}$$

$$\theta_0 = \frac{1}{1 + \exp\left(\frac{\phi-\phi_0}{b}\right)} \tag{6}$$

In this set of nonlinear differential equations the independent variables are ascribed as ϕ, the double layer potential; c, concentration changes of an electroactive species; θ, the surface coverage of a poisoning species; and ε, μ, and Γ as the time scales for ϕ, c, and θ, respectively. E is defined as the applied voltage, and ρ is the total resistance under potentiostatic control. k represents the reaction rate constant with a cubic dependency on ϕ, and θ_0 describes a sigmoidal curve of the poison coverage derived by a Langmuir isotherm with b and ϕ_0

as constants. Both k and θ_0 represent the steady states as a function of the double layer potential.

The effect of the cation on the overall reaction rate during the electro-oxidation of ethylene glycol was implemented by an inclusion of a Gaussian function to represent its steady state,

$$\theta_{0,c} = \lambda \exp\left[-\frac{(\phi-\delta)^2}{2\sigma^2}\right] \tag{7}$$

Hence, $\theta_{0,c}$ represents the steady states for the cation coverage; λ is the highest degree of coverage reached; δ is the position in terms of ϕ at the highest coverage; and σ is the standard deviation that can be also interpreted as the peak width. The proper choice for this function was rationalized in terms of noncovalent interactions between the hydrated alkali cations and surface oxygenated species formed in high potentials. In this context, the cation coverage might be favored when the potential increases, because of the formation of platinum oxides, and then be taken away from the surface by electrostatic repulsion when larger positive charge density is accumulated in high potentials on the surface.

The set of eqs 2−6 can be modified by the inclusion of the cation coverage θ_c with its respective time scale of formation Γ_c as the following,

$$\varepsilon\frac{d\phi}{dt} = -c(1-\theta-\theta_c)k + \frac{E-\phi}{\rho} \tag{8}$$

$$\mu\frac{dc}{dt} = -c(1-\theta-\theta_c)k - c + 1 \tag{9}$$

$$\Gamma\frac{d\theta}{dt} = \theta_0 - \theta \tag{10}$$

$$\Gamma_c\frac{d\theta_c}{dt} = \theta_{0,c} - \theta_c \tag{11}$$

in which

$$\theta_0 = \frac{1 - \theta_{0,c}}{1 + \exp\left(\frac{\phi-\phi_0}{b}\right)} \tag{12}$$

The mathematical model was integrated by a fourth order Runge−Kutta method with a fixed step of 0.005 in the commercially available software Matlab. The parameters used in these simulations are listed in Table 1.

The potential window, resistance, and initial double layer potential were selected from previous analysis in the literature,[42] while σ was optimized in order to enhance the cation inhibition and reproduce the experimental observations. With focus on the study of the hydrated alkali cation effect in the overall reaction rate, three different conditions were

Table 1. Parameters Used in the Numerical Simulations

ε	0.001
μ	50
b	7.12
δ	160
σ	60
E	238
condition A	$\Gamma = 0.5$, $\Gamma_c = 1.5$, and $\lambda = 0.05$
condition B	$\Gamma = 0.8$, $\Gamma_c = 1.1$ and $\lambda = 0.70$
condition C	$\Gamma = 0.9$, $\Gamma_c = 1.0$, and $\lambda = 1.00$

selected and are described in Table 1. The choice of parameters and numerical values was based on the following experimental observations: (a) smaller cations or larger hydration energies promoted a more efficient suppression on the faradaic current, and then it might correspond to higher values of λ and consequently lower values of Γ_c; (b) smaller cations also induced lower oscillatory frequencies due the blocking effect. In this case, it satisfies the same requirements of item a. Similar effect in the decrease of the frequency is also observed for the adsorption of poisoning species.[24,43] (c) The first order poisoning rate constant, k_p, seems to be mostly dependent on the formation of carbonaceous species in the platinum electrode, as experimentally observed. Clearly, there is an intricate combination between Γ, Γ_c, and λ in slowing the oscillations with a simultaneous inhibiting effect of the total reaction rate. In fact, these observations were tested and verified separately in our numerical simulations, and three different conditions with fixed parameters values were set in order to reproduce all experimental observations.

Condition A presents $\Gamma = 0.5$, $\Gamma_c = 1.5$, and $\lambda = 0.05$ which indicates the slowest formation and the weakest interaction of the hydrated cation in the supporting electrolyte with the surface oxides, besides the fastest rate of formation of the inhibitor. This case would correspond to KOH media. In addition, two more conditions were established: condition B and condition C. The former shows, as parameters, $\Gamma = 0.8$, $\Gamma_c = 1.1$, and $\lambda = 0.70$, and the latter, $\Gamma = 0.9$, $\Gamma_c = 1.0$, and $\lambda = 1.00$. Then conditions B and C would represent the NaOH and LiOH solutions, respectively. Overall, we adopted the formation of θ as always faster than θ_c. Nevertheless, as the cation effect gets stronger with larger λ, this difference in the kinetic rates decreases. Experimentally, this behavior is related to stronger noncovalent interactions that prevent the electro-oxidation of the organic intermediates with the oxygenated species on the surface, slowing the formation of θ by the production of lesser amounts of free active sites.

Figure 4 depicts linear potential sweeps calculated based on the set of four coupled nonlinear differential eqs 8−11, at $dE/dt = 3.25$ in the range of $50 < E < 230$ with $\rho = 1.0$ and $\phi_0 = 124.6$. As observed from the simulations, the difference among the total currents in the linear potential sweeps reflects the competition for free active sites between the inhibitor and hydrated alkali cation isotherms, resulting in diverse extensions of surface blocking. In Figure 4a, the peak current amounts to $I = 0.95$, 1.95, and 2.85 for conditions A, B, and C, and consequently, this current suppression is followed by an accumulation of the interfacial concentration of the electro-active species, as evidenced in Figure 4b. Note in Figure 4c and 4d that θ decreases as long the cation interacts stronger with adsorbed species at the surface, respectively.

As a dimensionless model, our simulations required numeric values to some parameters that are not necessarily found in real conditions. Indeed, values for λ can be considered extremely high for the cation coverage, but it still can be adopted as a suitable choice, since its precursor is related to the formation of platinum oxides. Considering more realistic models,[44,45] adsorbed carbon monoxide and platinum oxides coverages always go to 1.0 at low and high potential ranges, respectively. The difference in our model, however, is the adoption of an electrostatic repulsion at high potentials, described by the decay in the Gaussian curve after its maximum peak, which promotes the decrease of θ_c. Even so, this effect induces a slight increment of current when a stronger interaction is considered.
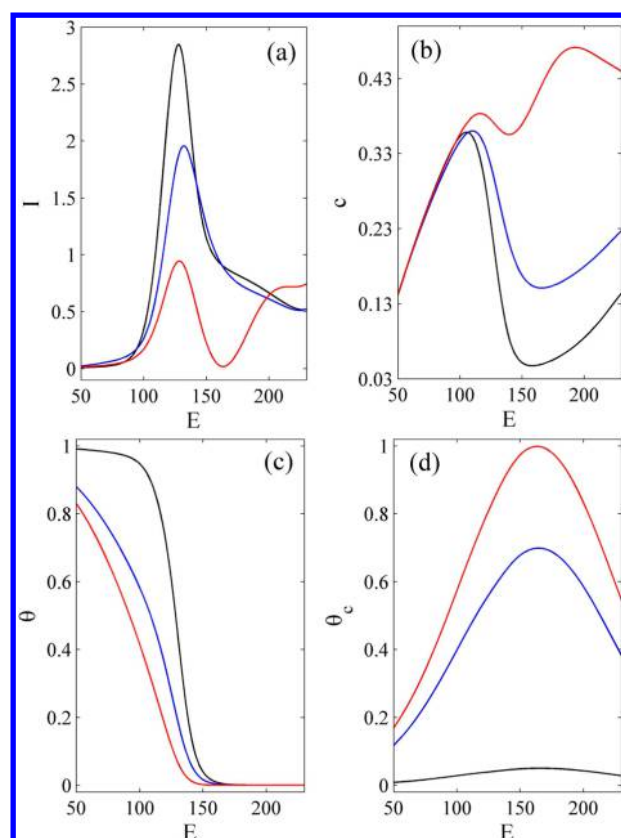

Figure 4. Linear potential sweeps at $dE/dt = 3.25$ in the range of $50 < E < 230$, $\rho = 1.0$, and $\phi_0 = 124.6$ with the condition A as black, condition B as blue, and condition C as red lines, respectively. (a) I, total current; (b) c, concentration; (c) θ, inhibitor coverage; (d) θ_c, cation coverage.

Voltages above 200 clearly exemplify this description. Numerical evidence shown in Figure 4a is in agreement with this catalytic enhancement at high potentials.

Figure 5 shows a set of time series collected at different resistances for $\phi_0 = 200$ and (a) condition C, (b) condition B, (c) condition A. With the aim of studying the cation effect in the potential oscillations, an increase of ϕ_0 to 200 allowed us to obtain mostly period 1 harmonic oscillations in a wide range of parameters. As already shown, this kind of waveform is a typical characteristic found in the EG electro-oxidation in alkaline media.[19−21] Period 1 oscillations were mostly observed in all conditions studied and overall smaller radius of the cations resulted in lower frequencies. At $\rho = 100$ it was observed in a descending sequence of $\omega_A = 0.97$, $\omega_B = 0.69$, and $\omega_C = 0.63$. The indexes A, B, and C in the frequencies indicate the type of each condition; see Table 1 for additional details. As also observed in the experiments, larger applied resistances (or galvanostatic control) resulted in relatively slight changes in the frequency. The numerical simulations provided a good semiquantitative approximation compared to the experimental observations: $\omega_{Li}/\omega_{Na} = 0.88$, $\omega_{Na}/\omega_K = 0.77$; and $\omega_C/\omega_B = 0.91$, $\omega_B/\omega_A = 0.71$ for $\rho = 100$.

Although all data treatment was realized focusing just on period 1 oscillations, the electrochemical experiments also revealed more complex temporal patterns, especially in the presence of Li$^+$ ions; see Figure 2 for instance. As previously discussed, the presence of the hydrated alkali cations in reaction media has an intricate effect on the overall reaction network. It
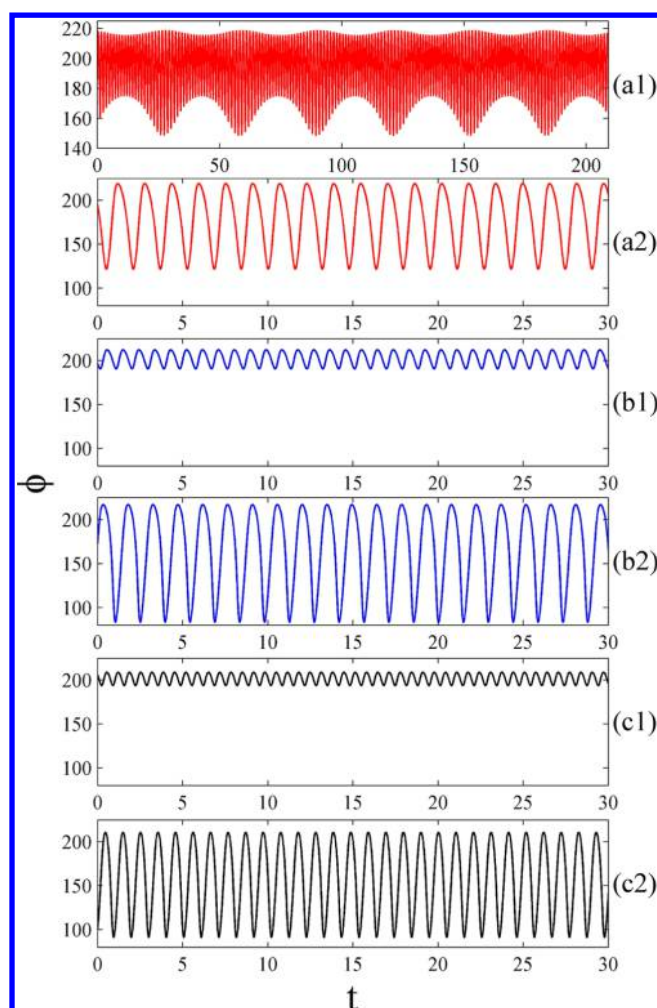
Figure 5. Potential time series for $\phi_0 = 200$. (a) Condition C as red lines, index 1: $\rho = 82$. Index 2: $\rho = 100$ and $\omega_C = 0.63$. (b) Condition B as blue lines, index 1: $\rho = 53$ and $\omega_B = 1.07$. Index 2: $\rho = 100$ and $\omega_B = 0.69$. (c) Condition A as black lines, index 1: $\rho = 45$ and $\omega_A = 1.51$. Index 2: $\rho = 100$ and $\omega_A = 0.97$.

can block the catalytic activity by the noncovalent interactions with surface oxides, which, in its turn, prevent the consumption of adsorbed carbonaceous residues, but simultaneously it is repelled from the surface due to positive−positive electrostatic interactions in high potentials. This puzzling mechanism might also result in complex temporal patterns, such as quasi-periodic behavior, mixed-mode oscillations, and chaos. In this context, we enhanced the cation effect on the dynamics, tuning λ to larger values. This means that in the potential window where the oscillations take place, a high degree and compact cation layer is favored. When this condition was satisfied, quasi-periodicity was observed in the range of approximately $77.5 < \rho < 83.6$; vide Figure 5a and index 1. Complicated periods 2, 3, 7 and irregular (potentially chaotic) waveforms were observed in condition C when σ was increased to 80 (data not shown). Considering just period 1 harmonic oscillations, we were able to numerically calculate the first order poisoning rate, $k_{p,n}$ described in eq 13,

$$\omega = \sqrt{\frac{k_{p,n}}{\varepsilon}\left(\frac{1}{\rho} + \frac{dI}{d\phi}\right)}\Bigg|_{\phi=\phi_{Hopf}} \qquad (13)$$

by the analysis of the dependency of the oscillatory frequency and the slope $dI/d\phi$, obtained in slow linear potential sweeps, under different resistances. The numerical results are shown in Figure 6. Similar procedure was adopted in Figure 3.
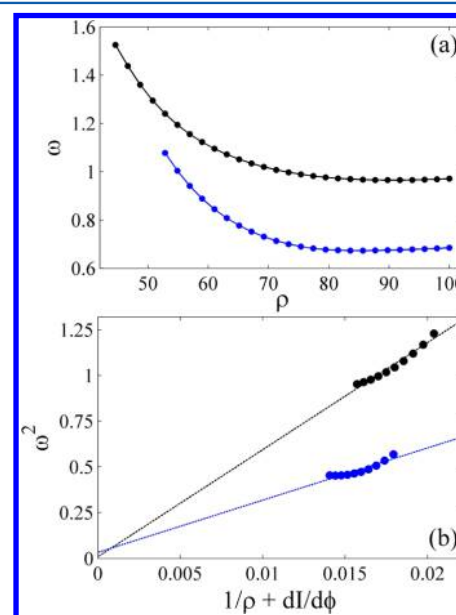

Figure 6. Simulated oscillatory frequency at $\phi_0 = 200$ close to the Hopf bifurcation as a function of (a) the external resistance, with condition A as black lines and condition B as blue lines, and (b) the quantity $1/\rho + dI/d\phi$ obtained from item a.

Figure 6a depicts a frequency decay when the resistance increases for two different conditions: A (black lines) and B (blue lines). Remarkably, the inhibition by the cation layer formation induced lower oscillatory frequencies in the range of $45 < \rho < 100$. On the basis of the theory proposed by Kiss et al.,[28,34] the numerically calculated reaction rate constants, extracted from eq 13 and shown in Figure 6b, were 5.85×10^4 and 2.85×10^4, with intercept coefficients of 0.008 and 0.057, R^2 values of 0.970 and 0.874 for the conditions A and B, respectively (nonlinear deviations appeared in very low or very high resistances). Again, the numerical simulations presented a good semiquantitative approximation compared to the electrochemical measurements: $k_{p,e-Na}/k_{p,e-K} = 0.45$ and $k_{p,n-B}/k_{p,n-A} = 0.49$. The difference between $k_{p,e}$ and $k_{p,n}$ reaction rate constants is that the former is an apparent constant once it has a dependency on the total free active sites. In fact, $k_{p,e}$ describes a series of composite reactions for C−C bond breaking and formation of carbonaceous intermediates. On the other hand, $k_{p,n}$ is related to one elementary step of formation of θ. Hence, the comparison between these rate constants can be done by adjustments in Γ, Γ_σ, and λ simultaneously.

4. CONCLUSIONS

Noncovalent interactions between hydrated alkali cations and negatively charged adsorbed species at the platinum surface play a decisive influence on the reaction rates and the electrochemical mechanism. In this work, we demonstrate this effect during the course of a complex reaction network in which the kinetic rates (and thus concentrations of intermediate species) exhibit a cyclic variation. Herein we gained some mechanistic insights into the effects of different types of alkali cations on the electro-oxidation of ethylene

glycol on platinum and in alkaline media. Besides the nontrivial effect on the oscillation waveform, we observed that the alkali cation causes the decrease of the oscillation frequency and of the poisoning rate constant, k_p, and this effect is more pronounced in the sequence $Li^+ > Na^+ > K^+$. The decrease of these two parameters occurs in the same direction of the decrease in the overall current density under nonoscillatory conditions.

The cation influence on the global reaction rate was modeled by an inclusion of a Gaussian curve to represent the steady state of its formation as a function of double layer potential in a dimensionless electrochemical oscillator of the HN-NDR class. Numerical simulations under potentiodynamic and oscillatory regimes were carried out, and a good semiquantitative and qualitative agreement were obtained. The effect of cation inhibition found here is essentially different from that commonly found for electrosorbing anions in acidic media. The mechanistic changes, due to the noncovalent interactions, have been rationalized in terms of the interfacial concentration of $PtOH-M^+(H_2O)_x$ clusters and also of the organic adsorbates. Indeed, k_p corresponds to the C−C bond breaking in the EG electro-oxidation, and the inhibition caused by the hydrated alkali cation is associated with the prevention of the electrochemical reaction between carbonaceous intermediates with oxygenated species. In addition, experimental and numerical observations indicate that small cations might induce complex temporal patterns. Finally, besides completing our investigation on the role of alkali cations in the electro-oxidation of ethylene glycol,[10] this contribution widens our (presently simplistic) knowledge of the relationship between the mechanism under regular and oscillatory regimes and opens some perspectives for future investigations.

■ AUTHOR INFORMATION

Corresponding Authors
*E.S.: e-mail, esitta@ufscar.br.
*H.V.: e-mail, varela@iqsc.usp.br.

Notes
The authors declare no competing financial interest.

■ ACKNOWLEDGMENTS

■ REFERENCES

(1) Tripkovic, D. V.; Strmcnik, D.; van der Vliet, D.; Stamenkovic, V.; Markovic, N. M. The Role of Anions in Surface Electrochemistry. *Faraday Discuss.* **2008**, *140*, 25−40.

(2) Iwasita, T. Methanol and CO Electro-Oxidation. In *Handbook of Fuel Cells: Fundamentals, Technology and Applications*; Vielstich, W., Lamm, A., Gasteiger, H. A., Eds.; John Wiley & Sons: Chichester, U.K., 2003; Vol. 2, pp 603−624.

(3) Lai, S. C. S.; Koper, M. T. M. The Influence of Surface Structure on Selectivity in the Ethanol Electro-Oxidation Reaction on Platinum. *J. Phys. Chem. Lett.* **2010**, *1*, 1122−1125.

(4) Batista, E. A.; Malpass, G. R. P.; Motheo, A. J.; Iwasita, T. New Mechanistic Aspects of Methanol Oxidation. *J. Electroanal. Chem.* **2004**, *571*, 273−282.

(5) Cuesta, A. At Least Three Contiguous Atoms Are Necessary for CO Formation during Methanol Electrooxidation on Platinum. *J. Am. Chem. Soc.* **2006**, *128*, 13332−13333.

(6) Strmcnik, D.; Escudero-Escribano, M.; Kodama, K.; Stamenkovic, V. R.; Cuesta, A.; Markovic, N. M. Enhanced Electrocatalysis of the Oxygen Reduction Reaction Based on Patterning of Platinum Surfaces with Cyanide. *Nat. Chem.* **2010**, *2*, 880−885.

(7) Strmcnik, D.; Kodama, K.; van der Vliet, D.; Greeley, J.; Stamenkovic, V. R.; Markovic, N. M. The Role of Non-Covalent Interactions in Electrocatalytic Fuel-Cell Reactions on Platinum. *Nat. Chem.* **2009**, *1*, 466−472.

(8) Stoffelsma, C.; Rodriguez, P.; Garcia, G.; Garcia-Araez, N.; Strmcnik, D.; Markovic, N. M.; Koper, M. T. M. Promotion of the Oxidation of Carbon Monoxide at Stepped Platinum Single-Crystal Electrodes in Alkaline Media by Lithium and Beryllium cations. *J. Am. Chem. Soc.* **2010**, *132*, 16127−16133.

(9) Previdello, B. A. F.; Machado, E. G.; Varela, H. The Effect of the Alkali Metal Cation on the Electrocatalytic Oxidation of Formate on Platinum. *RSC Adv.* **2014**, *4*, 15271−15275.

(10) Sitta, E.; Batista, B. C.; Varela, H. The Impact of the Alkali Cation on the Mechanism of the Electro-Oxidation of Ethylene Glycol on Pt. *Chem. Commun.* **2011**, *4*, 3775−3777.

(11) Angelucci, C. A.; Varela, H.; Tremiliosi, G.; Gomes, J. F. The Significance of Non-Covalent Interactions on the Electro-Oxidation of Alcohols on Pt and Au in Alkaline Media. *Electrochem. Commun.* **2013**, *33*, 10−13.

(12) Katsounaros, I.; Mayrhofer, K. J. J. The Influence of Non-Covalent Interactions on the Hydrogen Peroxide Electrochemistry on Platinum in Alkaline Electrolytes. *Chem. Commun.* **2012**, *48*, 6660−6662.

(13) Mills, J. N.; McCrum, I. T.; Janik, M. J. Alkali Cation Specific Adsorption onto fcc(111) Transition Metal Electrodes. *Phys. Chem. Chem. Phys.* **2014**, *16*, 13699−13707.

(14) Matanović, I.; Atanassov, P.; Garzon, F. H.; Henson, N. J. Density Functional Theory Study of the Alkali Metal Cation Adsorption on Pt(111), Pt(100), and Pt(110) Surfaces. *ECS Trans.* **2014**, *61*, 47−53.

(15) Krischer, K.; Varela, H. Oscillations and Other Dynamic Instabilities. In *Handbook of Fuel Cells: Fundamentals, Technology and Applications*; Vielstich, W., Lamm, A., Gasteiger, H. A., Eds.; John Wiley & Sons: Chichester, U.K., 2003; Vol. 2, pp 679−701.

(16) Krischer, K. Nonlinear Dynamics in Electrochemical Systems. In *Advances in Electrochemical Science and Engineering*; Alkire, R. C., Kolb, D. M., Eds.; Wiley-VCH: Weinheim, Germany, 2003; Vol. 8, pp 90−203.

(17) Koper, M. T. M. The Theory of Electrochemical Instabilities. *Electrochim. Acta* **1992**, *37*, 1771−1778.

(18) Strasser, P.; Eiswirth, M.; Koper, M. T. M. Mechanistic Classification of Electrochemical Oscillators—Operational Experimental Strategy. *J. Electroanal. Chem.* **1999**, *478*, 50−66.

(19) Sitta, E.; Nascimento, M. A.; Varela, H. Complex Kinetics, High Frequency Oscillations and Temperature Compensation in the Electro-Oxidation of Ethylene Glycol on Platinum. *Phys. Chem. Chem. Phys.* **2010**, *12*, 15195−15206.

(20) Sitta, E.; Varela, H. Beta Oscillations in the Electro-Oxidation of Ethylene Glycol on Platinum. *Electrocatal.* **2010**, *1*, 19−21.

(21) Sitta, E.; Nagao, R.; Varela, H. The Electro-Oxidation of Ethylene Glycol on Platinum Over a Wide pH Range: Oscillations and Temperature Effects. *PLoS One* **2013**, *8*, e75086.

(22) Hachkar, M.; Beden, B.; Lamy, C. Oscillating Electrocatalytic Systems. 1. Survey of Systems Involving the Oxidation of Organics and Detailed Electrochemical Investigation of Formaldehyde Oxidation on Rhodium Electrodes. *J. Electroanal. Chem.* **1990**, *287*, 81−98.

(23) Oliveira, C. P.; Lussari, N. V.; Sitta, E.; Varela, H. Oscillatory Electro-Oxidation of Glycerol on Platinum. *Electrochim. Acta* **2012**, *85*, 674−679.

(24) Ferreira, G. C. A.; Batista, B. C.; Varela, H. Experimental Assessment of the Sensitiveness of an Electrochemical Oscillator towards Chemical Perturbations. *PLoS One* **2012**, *7*, e50145.

(25) Chen, S. L.; Noles, T.; Schell, M. Differences in Oscillations and Sequences of Dynamical States Caused by Anion Adsorption in the Electrochemical Oxidation of Formic Acid. *J. Phys. Chem. A* **2000**, *104*, 6791−6798.

(26) Swamy, B. E. K.; Vannoy, C.; Maye, J.; Kamali, F.; Huynh, D.; Little, B. B.; Schell, M. Potential Oscillations in Formic Acid Oxidation in Electrolyte Mixtures: Efficiency and Stability. *J. Electroanal. Chem.* **2009**, *625*, 69−74.

(27) Chen, S. L.; Noles, T.; Schell, M. Effects of Anions on Chemical Instabilities in the Oxidation of Formic Acid. *Electrochem. Commun.* **2000**, *2*, 171−174.

(28) Kiss, I. Z.; Sitta, E.; Varela, H. On the Limit of Frequency of Electrochemical Oscillators and Its Relationship to Kinetic Parameters. *J. Phys. Chem. C* **2012**, *116*, 9561−9567.

(29) Malkhandi, S.; Bonnefont, A.; Krischer, K. Dynamic Instabilities during the Continuous Electro-Oxidation of CO on Poly- and Single Crystalline Pt Electrodes. *Surf. Sci.* **2009**, *603*, 1646−1651.

(30) Malkhandi, S.; Bauer, P. R.; Bonnefont, A.; Krischer, K. Mechanistic Aspects of Oscillations during CO Electrooxidation on Pt in the Presence of Anions: Experiments and Simulations. *Catal. Today* **2013**, *202*, 144−153.

(31) Okamoto, H.; Kikuchi, M.; Mukouyama, Y. Effect of Chloride Ions on Potential Oscillation Generated by Formic Acid Oxidation. *J. Electroanal. Chem.* **2008**, *622*, 1−9.

(32) Mukouyama, Y.; Nakanishi, S.; Konishi, H.; Nakato, Y. Electrochemical Oscillations of a New Type in an H_2O_2 + H_2SO_4 Vertical Bar Pt-Electrode System, Appearing by Addition of Small Amounts of Halide Ions. *J. Electroanal. Chem.* **1999**, *473*, 156−165.

(33) Nagao, R.; Cantane, D. A.; Lima, F. H. B.; Varela, H. Influence of Anion Adsorption on the Parallel Reaction Pathways in the Oscillatory Electro-Oxidation of Methanol. *J. Phys. Chem. C* **2013**, *117*, 15098−15105.

(34) Kiss, I. Z.; Pelster, L. N.; Wickramasinghe, M.; Yablonsky, G. S. Frequency of Negative Differential Resistance Electrochemical Oscillators: Theory and Experiments. *Phys. Chem. Chem. Phys.* **2009**, *11*, 5720−5728.

(35) Housmans, T. H. M.; Koper, M. T. M. Methanol Oxidation on Stepped Pt *n*(111) × (110) Electrodes: A Chronoamperometric Study. *J. Phys. Chem. B* **2003**, *107*, 8557−8567.

(36) Grozovski, V.; Climent, V.; Herrero, E.; Feliu, J. M. Intrinsic Activity and Poisoning Rate for HCOOH Oxidation at Pt(100) and Vicinal Surfaces Containing Monoatomic (111) Steps. *ChemPhysChem* **2009**, *10*, 1922−1926.

(37) Christensen, P. A.; Hamnett, A. The Oxidation of Ethylene Glycol at a Platinum Electrode in Acid and Base: An in Situ FTIR Study. *J. Electroanal. Chem.* **1989**, *260*, 347−359.

(38) Chang, S. C.; Ho, Y. H.; Weaver, M. J. Applications of Real Time FTIR Spectroscopy to the Elucidation of Complex Eectroorganic Pathways—Electro-Oxidation of Ethylene Glycol on Gold, Platinum, and Nickel in Alkaline Solution. *J. Am. Chem. Soc.* **1991**, *113*, 9506−9513.

(39) Krischer, K. Principles of Temporal and Spatial Pattern Formation in Electrochemical Systems. In *Modern Aspects of Electrochemistry*; Conway, B. E., Bockris, J. O., White, R. E., Eds.; Kluver Academic/Plenum Publishers: New York, 1999; Vol. *32*, pp 1−142.

(40) Koper, M. T. M.; Sluyters, J. H. Electrochemical Oscillators—Their Description through a Mathematical Model. *J. Electroanal. Chem.* **1991**, *303*, 73−94.

(41) Koper, M. T. M.; Sluyters, J. H. Instabilities and Oscillations in Simple-Models of Electrocatalytic Surfaces Reactions. *J. Electroanal. Chem.* **1994**, *371*, 149−159.

(42) Nascimento, M. A.; Gallas, J. A. C.; Varela, H. Self-Organized Distribution of Periodicity and Chaos in an Electrochemical Oscillator. *Phys. Chem. Chem. Phys.* **2011**, *13*, 441−446.

(43) Batista, B. C.; Ferreira, G. C. A.; Varela, H. The Effect of Poisoning Species on the Oscillatory Dynamics of an Electrochemical Reaction. *J. Phys.: Conf. Ser.* **2011**, *285*, 012003.

(44) Strasser, P.; Eiswirth, M.; Ertl, G. Oscillatory Instabilities during Formic Acid Oxidation on Pt(100), Pt(110) and Pt(111) under Potentiostatic Control. 2. Model Calculations. *J. Chem. Phys.* **1997**, *107*, 991−1003.

(45) Zhang, J. X.; Datta, R. Sustained Potential Oscillations in Proton Exchange Membrane Fuel Cells with PtRu as Anode Catalyst. *J. Electrochem. Soc.* **2002**, *149*, A1423−A1431.